



RESEARCH ARTICLE

10.1029/2019EF001473

Key Points:

- Five compound climate extremes are projected to be more frequent in Africa under both emission scenarios by the end of the century
- Populations in West Africa, Central-East Africa, and Northeast and Southeast Africa are projected to be particularly exposed
- Increased exposure is mainly driven by the interaction between climate and population growth, and the effect of population alone

Supporting Information:

- Supporting Information S1
- Table S1

Correspondence to:

T. Weber,
torsten.weber@hzg.de

Citation:

Weber, T., Bowyer, P., Rechid, D., Pfeifer, S., Raffaele, F., Remedio, A. R., et al. (2020). Analysis of compound climate extremes and exposed population in Africa under two different emission scenarios. *Earth's Future*, 8, e2019EF001473. <https://doi.org/10.1029/2019EF001473>

Received 31 DEC 2019

Accepted 11 AUG 2020

Accepted article online 16 AUG 2020

[Correction added on 24 SEP 2020, after first online publication: Projekt Deal funding statement has been added.]

Analysis of Compound Climate Extremes and Exposed Population in Africa Under Two Different Emission Scenarios

T. Weber¹ , P. Bowyer¹ , D. Rechid¹, S. Pfeifer¹, F. Raffaele², A. R. Remedio¹ , C. Teichmann¹ , and D. Jacob¹

¹Climate Service Center Germany (GERICS), Helmholtz-Zentrum Geesthacht, Hamburg, Germany, ²Abdus Salam International Centre for Theoretical Physics, Trieste, Italy

Abstract It is well established that Africa is particularly exposed to climate extremes including heat waves, droughts, and intense rainfall events. How exposed Africa is to the co-occurrence of these events is however virtually unknown. This study provides the first analysis of projected changes in the co-occurrence of five such compound climate extremes in Africa, under a low (RCP2.6) and high (RCP8.5) emissions scenario. These changes are combined with population projections for a low (SSP1) and high (SSP3) population growth scenario, in order to provide estimates of the number of people that may be exposed to such events at the end of the 21st century. We make use of an ensemble of regional climate projections from the Coordinated Output for Regional Evaluations (CORE) project embedded in the Coordinated Regional Climate Downscaling Experiment (CORDEX) framework. This ensemble comprises five different Earth System Model/Regional Climate Model (ESM/RCM) combinations with three different ESMs and two RCMs. We show that all five compound climate extremes will increase in frequency, with changes being greater under RCP8.5 than RCP2.6. Moreover, populations exposed to these changes are greater under RCP8.5/SSP3, than RCP2.6/SSP1, increasing by 47- and 12-fold, respectively, compared to the present-day. Regions of Africa that are particularly exposed are West Africa, Central-East Africa, and Northeast and Southeast Africa. Increased exposure is mainly driven by the interaction between climate and population growth, and the effect of population alone. This has important policy implications in relation to climate mitigation and adaptation.

Plain Language Summary It is well known that Africa is exposed to a range of different climate hazards including droughts, heat waves, and extreme rainfall events, which cause major social and economic suffering. It is, however, largely unknown how exposed the African population is to the co-occurrence of such climate hazards. This is important because compound events will likely increase the suffering far and above that caused by individual climate hazards. In this study, we provide an analysis of potential changes in five different compound events, and the exposure of the African population to them, at the end of this century. Combining exposure to all compound events, the results show that compared to the present-day, the exposure of the African population may increase by 12- and 47-fold in the best- and worst-case scenarios, respectively. The spatial distribution of changes shows that West Africa and central and eastern regions of Africa may be particularly exposed. Increased exposure is mainly caused by the interaction between climate and population growth, and the effect of population alone. These results imply that any policy response designed to reduce exposure needs to address both climatic and socioeconomic factors.

1. Introduction

Africa is particularly exposed and vulnerable to a wide range of different climate risks (Chersich et al., 2018; Dosio, 2017; Hummel et al., 2018; Niang et al., 2014; Russo et al., 2016; Thornton et al., 2011). Policymakers seeking to understand the climate risks faced by Africa in a changing climate therefore need information on the climate hazards, exposure of assets, and vulnerability, if they are to plan and adapt effectively. To date, the vast majority of climate risk assessments have investigated the risk posed by individual climate hazards; however, there is significant evidence to show that this approach is incomplete and that the impacts resulting from the interplay and combination of a number of climate drivers and/or hazards often result in much

©2020. The Authors. Earth's Future published by Wiley Periodicals LLC on behalf of American Geophysical Union. This is an open access article under the terms of the Creative Commons Attribution License, which permits use, distribution and reproduction in any medium, provided the original work is properly cited.

larger impacts than consideration of individual hazards in isolation (Leonard et al., 2014; Zscheischler et al., 2018). As such, failing to provide analysis of these compound events is likely to underestimate the risk posed by climate impacts and thus will lead to inadequate adaptation planning (Hendry et al., 2019; Turner et al., 2019).

Seneviratne et al. (2012) define such compound climate events as follows: “(1) two or more extreme events occurring simultaneously or successively, (2) combinations of extreme events with underlying conditions that amplify the impact of the events, or (3) combinations of events that are not themselves extremes but lead to an extreme event or impact when combined.” Zscheischler et al. (2018) subsequently generalized this definition to “the combination of multiple drivers, and/or hazards that contributes to societal or environmental risk.”

Historically, there has been very little attention devoted to the analysis of compound climate events; however, recent years have seen a starburst of activity with a number of papers investigating compound climate events. For example, the co-occurrence of hot and dry periods (AghaKouchak et al., 2014; Feng et al., 2019; Hao et al., 2018; Lu et al., 2018; Manning et al., 2019; Mazdiyasi & AghaKouchak, 2015), temporally compound heat waves (Baldwin et al., 2019), compound coastal flooding (Hendry et al., 2019; Sadegh et al., 2018; Wahl et al., 2015), tropical cyclones and deadly heat (Matthews et al., 2019), wind and precipitation extremes (Martius et al., 2016), wildfire and extreme rainfall (Moftakhari & AghaKouchak, 2019), and temperature and precipitation extremes (Turner et al., 2019; Zscheischler & Seneviratne, 2017).

This increase in activity notwithstanding, there is a real dearth of information on compound climate events that the African continent may face in the future. The analysis by Hao et al. (2018), which provided a global analysis of observed changes in the severity of compound dry and hot extremes, is the only research that provides any information, with Africa being one of the regions of the world that has seen a significant increase in this type of compound event.

Given that there is evidence to show that changes in climate extremes as well as compound climate extremes may increase in the future, makes it all the more important to analyze changes in compound events in Africa (Kendon et al., 2019; Liu et al., 2017; Sedlmeier et al., 2016). This need is made all the greater still when one considers that the African continent is witnessing rapid population growth, which will continue through to the end of this century, with the population of sub-Saharan Africa projected to double by 2050, and reach almost 3.8 billion by 2100 (UN, 2019). As such, policymakers responsible for adaptation planning will clearly be facing increasing risks over the course of this century.

Various studies have investigated the future exposure of the African population to climate hazards using climate models and projections of population. Liu et al. (2017), in a global analysis of future exposure to heat wave days for various emissions scenarios and population projections, showed that the average exposure for the African continent by the end of the century was over 118 times greater than the present-day situation. Asefi-Najafabady et al. (2018) in an analysis of exposure to apparent temperature above 39°C in the Great Lakes region of Africa showed that the largest increases in exposure were in low lying areas of Kenya, Uganda, and the Democratic Republic of Congo. Harrington and Otto (2018) analyzed changes in extreme heat using a single climate model and a range of population projections, for two different global warming levels, and showed that for the east African subregion there may be a fivefold increase in extreme heat exposure in a 2°C versus a 1.5°C warmer world. Ahmadalipour et al. (2019) analyzed changes in drought risk at the national level across Africa and showed that all countries would see an increase in drought risk, with Niger and Chad the two most at risk countries. Rohat et al. (2019) investigated exposure to dangerous heat in 173 large African cities and showed that exposure may increase by a multiple of 20–52 by the 2090s. All these studies investigate exposure to a single climate hazard. To the best of our knowledge, there are no studies that analyze future changes in exposure to compound climate events for Africa.

In this study we make use of high-resolution regional climate projections from the newly performed Coordinated Output for Regional Evaluations (CORE) embedded in the Coordinated Regional Climate Downscaling Experiment (CORDEX) framework (e.g., Ciarlo et al., 2020; Remedio et al., 2019), to investigate changes in five different compound climate extremes, which we combine with population projection data to calculate exposed populations at the end of the century. This study represents the first analysis of its kind for Africa.

The rest of this paper is structured as follows: Initially, the data and methods used in the study are described in section 2; the results are described in section 3; while section 4 provides a discussion of the results; and finally, in section 5 we make some conclusions.

2. Materials and Methods

2.1. Climate Reanalysis Data and Regional Climate Model Ensemble

In this work, the ERA5 reanalysis data set at a spatial resolution of 0.25° (~ 28 km) from the Copernicus Climate Change Service (C3S) (2017) is used to calculate the compound climate extremes for the reference period 1981–2010. To estimate the potential changes in these events for the future, the newly performed regional climate projections from Coordinated Output for Regional Evaluations (CORE) embedded in the Coordinated Regional Climate Downscaling Experiment (CORDEX) framework for Africa are applied (e.g., Ciarlo et al., 2020; Remedio et al., 2019). In order to take into account a low and a high emission scenario, the Representative Concentration Pathways (RCPs) 2.6 and 8.5 (Moss et al., 2010) are analyzed for the period 2070–2099. The model ensemble comprises five different Earth System Model/Regional Climate Model (ESM/RCM) combinations with three ESMs and two RCMs at a spatial resolution of 0.22° : MPI-ESM-LR/REMO2015, HadGEM2-ES/REMO2015, NorESM1-M/REMO2015, HadGEM2-ES/RegCM4-7, and NorESM1-M/RegCM4-7. In order to perform the analysis on a consistent spatial unit, these data were regridded to the same 0.25° resolution of the ERA5 data. The ESMs from Coupled Model Intercomparison Projects Phase 5 (CMIP5) (Taylor et al., 2012) are selected in a way to cover a large range of climate sensitivities. The regional climate models REMO and RegCM have been evaluated and applied in numerous studies for Africa (e.g., Abba Omar & Abiodun, 2017; Diallo et al., 2015; Diasso & Abiodun, 2017; Endris et al., 2013; Fotso-Nguemo, Vondou, Pokam, et al., 2017; Fotso-Nguemo, Vondou, Tchawoua, et al., 2017; Giorgi et al., 2012; Klutse et al., 2016; Ogwang et al., 2016; Tamoffo et al., 2019; Tang et al., 2019; Weber et al., 2018) and other regions (e.g., Coppola et al., 2014; Giorgi et al., 2014; Jacob et al., 2012; Remedio et al., 2019; Teichmann et al., 2013).

2.2. Population Data

To estimate the African population exposed to compound climate extremes for the reference period, the annual population data from the Inter-Sectoral Impact Model Intercomparison Project (ISIMIP) protocol ISIMIP2b (<https://www.isimip.org>) covering the period 1981–2005 at a spatial resolution of 5 arc-minutes ($\sim 0.083^\circ$) is employed. Due to the fact that the ISIMIP2b population data are only available until the end of 2005, the calculated population average comprises only 25 years for the reference period. For the scenario period, the future population is derived from the projections based on the Shared Socioeconomic Pathways (SSPs) provided by the NASA Socioeconomic Data and Applications Center (SEDAC) at a spatial resolution of 7.5 arc-minutes (0.125°) (Jones & O'Neill, 2016, 2017). Because of the fact that the population number is given at 10-year intervals, we calculated the mean over the years 2070, 2080, 2090, and 2100 from the SSPs for the scenario period 2070–2099. Both data sets were again regridded to a common 0.25° resolution in order to be able to integrate them with the climate data. In order to provide an analysis of a best- and worst-case scenario, we use a stringent mitigation emissions scenario together with a low population growth scenario (RCP2.6/SSP1), and a continued growth in global carbon emissions scenario and rapid population growth scenario (RCP8.5/SSP3). We decided to use the combination of RCP2.6/SSP1 and RCP8.5/SSP3 in our investigation based on the work by Liu et al. (2017), who consider other combinations unlikely.

2.3. Methods

2.3.1. Definition of Hazards

Three different temperature and precipitation extremes were selected to detect their simultaneous occurrence for present, and for future climate conditions under the RCP2.6 and RCP8.5 emission scenarios. For the calculation of heat waves, we used the description of Liu et al. (2017), who defined heat waves as three or more consecutive days with a temperature above the 95th percentile of the daily maximum temperature of the reference period. If the 95th percentile is lower than 25°C , the threshold is set to 25°C . In order to take into account precipitation climate extremes, we defined a meteorological drought as five or more consecutive days with a daily precipitation less than 1 mm and extreme precipitation with precipitation above the 95th percentile of precipitation on wet days (≥ 1 mm) of the reference period. Grid boxes with less than 100 wet days in 30 years were excluded for the calculation of extreme precipitation events to ensure a

Table 1
Overview of Analyzed Compound Events, Their Associated Societal Impacts, and Relevant Research Examples From the Literature

Compound event	Societal impacts	Relevant literature
Coincident heat waves and droughts	Many societal impacts are related to this compound event including, increased risk of wildfire, water availability problems, human mortality, impact on energy supplies, and crop production	Sedlmeier et al. (2018), Hao et al. (2018), Wu et al. (2019), Ye et al. (2019)
Coincident heat waves and extreme precipitation	Less is known about the potential impact of these compound events, but flash flooding is one potential impact	Tencer et al. (2016)
Sequential droughts and extreme precipitation	Less is known about the potential impact of these compound events, but flash flooding is one potential impact	He and Sheffield (2020)
Sequential heat waves and droughts	Many societal impacts are related to this compound event including, increased risk of wildfire, water availability problems, human mortality, impact on energy supplies, and crop production	AghaKouchak et al. (2014)
Sequential heat waves and extreme precipitation	Less is known about the potential impact of these compound events, but flash flooding is one potential impact	Tencer et al. (2016)

reasonable determination of the 95th percentile. The time series of climate extremes were calculated with the ERA5 reanalysis data set and with the five regional climate change projections under each emission scenario. Because the occurrence of wet days is different in the ERA5 and two scenario-driven regional climate projection data sets, there are differences in the areas that are excluded from analysis. This can be seen in Figures 2a–2f, 3a–3c, 3g–3i, 5d–5f, 7a–7c, and 7g–7i.

2.3.2. Definition of Compound Events

For the investigation of compound climate extremes, we take the definition by Zscheischler et al. (2018), who consider compound climate events as a combination of multiple drivers and/or hazards that contribute to societal or environmental risk and specify it as follows: Compound climate extremes comprise a combination of two different climate extremes that can occur coincidentally (simultaneously) or sequentially within a certain time period and that contribute to social or environmental risk. In detail, a coincident compound event takes place when two different climate extremes overlap one or more days. A sequential compound event occurs when an extreme event starts within 7 days after the termination of a preceding extreme event. Adopting the typology described in Zscheischler et al. (2020), the coincident events that we analyze are multivariate compound climate events, and the sequential events are temporally compounding climate events. Specifically, we analyze the following five different compound climate extremes (hereafter referred to as compound events):

1. Coincident heat waves and droughts: at least three consecutive days when the maximum temperature is above the 95th percentile value from the reference period (and this value must be greater than 25°C), combined with at least five consecutive days where daily precipitation is less than 1 mm.
2. Coincident heat waves and extreme precipitation: at least three consecutive days when the maximum temperature is above the 95th percentile value from the reference period (and this value must be greater than 25°C), combined with days when precipitation on wet days (≥ 1 mm) is above the 95th percentile value from the reference period.
3. Sequential droughts and extreme precipitation: at least five consecutive days when daily precipitation is less than 1 mm, followed, within 7 days, by days when precipitation on wet days (≥ 1 mm) is above the 95th percentile value from the reference period.
4. Sequential heat waves and droughts: at least three consecutive days when the maximum temperature is above the 95th percentile value from the reference period (and this value must be greater than 25°C), followed, within 7 days, by at least five consecutive days where daily precipitation is less than 1 mm.
5. Sequential heat waves and extreme precipitation: at least three consecutive days when the maximum temperature is above the 95th percentile value from the reference period (and this value must be greater than 25°C), followed, within 7 days, by days when precipitation on wet days (≥ 1 mm) is above the 95th percentile value from the reference period.

This combination of compound events was analyzed because of the wide-ranging number of societal impacts that they are associated with in the agriculture, water, infrastructure, and health sectors (Table 1). For each compound event, the occurrence was detected, and the overlapping days for the coincident events were calculated with the ERA5 reanalysis data set (for the reference period) and the regional climate change

projections (for the reference and future time period). Projected changes were then calculated for each climate model, and scenario combination. To aid interpretability, we present the results as the multimodel mean number of compound events per year, in each 30-year climate period. To obtain the total number of events occurring within a 30-year period, the frequencies have to be multiplied by 30. Additionally, to provide a basic assessment of the robustness of the results, we provide information on the level of model agreement based on the sign of the change. Model agreement is classified as high, if at least four out of the five model simulations are in agreement.

2.3.3. Exposure to Compound Events

In order to calculate exposed population to the compound events, we multiply the population by the number of compound events in each grid cell, for both the reference and future time periods, and refer to this metric as person-events. We also investigate the relative importance of the different drivers of change in exposure by using the approach first developed by Jones et al. (2015) and subsequently applied by Liu et al. (2017). Change in exposure (ΔE) is defined as being the sum of the climate, population, and interaction effect as follows:

$$\Delta E = P_R \times \Delta C + C_R \times \Delta P + \Delta C \times \Delta P, \quad (1)$$

where P_R and C_R denote the population and the climate in the reference period and ΔC and ΔP represent the climate and the population change in the scenario period, respectively. The first term of 1 describes the climate effect, which takes into account the influence of climate exposure, and the second one measures the population effect. The last term considers the combined impacts (interaction) of simultaneous change in both climate and population.

We analyze the changes in exposure, and the relative importance of the different drivers of change, for the different subregions of Africa. We make use of the new updated IPCC reference regions for the African continent (Iturbide et al., 2020), as follows: Sahara (SAH), West Africa (WAF), Central Africa (CAF), Northeast Africa (NEAF), Central-East Africa (CEAF), Southwest Africa (SWAF), Southeast Africa (SEAF), and a new defined region covering North Africa (NAF).

3. Results

To aid understanding of the results, all the values that we report in this section, both with respect to the compound events for the future time period, and the change in exposure, and relative importance of the drivers of change in exposure, are based on the multimodel mean values, unless otherwise stated. Also, to assist with interpretation of the spatial patterns of change, we provide a topographical map of Africa in Figure S1 in the supporting information, upon which the different countries of Africa are also labeled. A full breakdown of the information relating to the exposure, and the relative importance of the drivers, in both the reference and future time periods, including information on the range of uncertainty in the changes, is provided in Tables S1–S23.

3.1. Coincident Climate Extremes

3.1.1. Heat Waves and Droughts

In the climate reference period (1981–2010), coincident heat waves and droughts occur on average 1.2 to 2.5 times per year, over almost the entire African continent. Exceptions are the equatorial regions from the West Coast to Central Africa, the coastal regions of Southeast Africa, and East Madagascar with 0.06 to 1 times per year, or 1.8 to 30 times in a 30-year period (Figure 1a). This pattern is mainly caused by fewer heat waves in these regions. For the RCP2.6 scenario, the models project an increase of between 0 and 6 compound events per year (Figure 1b), and for the RCP8.5 emission scenario demonstrates a stronger increase of between 2 and 16 events per year, partly more, for the continent (Figure 1c). The most affected regions are located along 15°N, East Africa and Southern Africa. Both scenarios exhibit high model agreement for the entire continent. This compound event has an overlap duration of about 2 to 8 days for the reference period (Figure 1d) that extends by up to 7 days for RCP2.6 (Figure 1e) and by between 1 and 21 days for RCP8.5 (Figure 1f) with high model agreement for most regions under RCP2.6 and for the whole of Africa under RCP8.5.

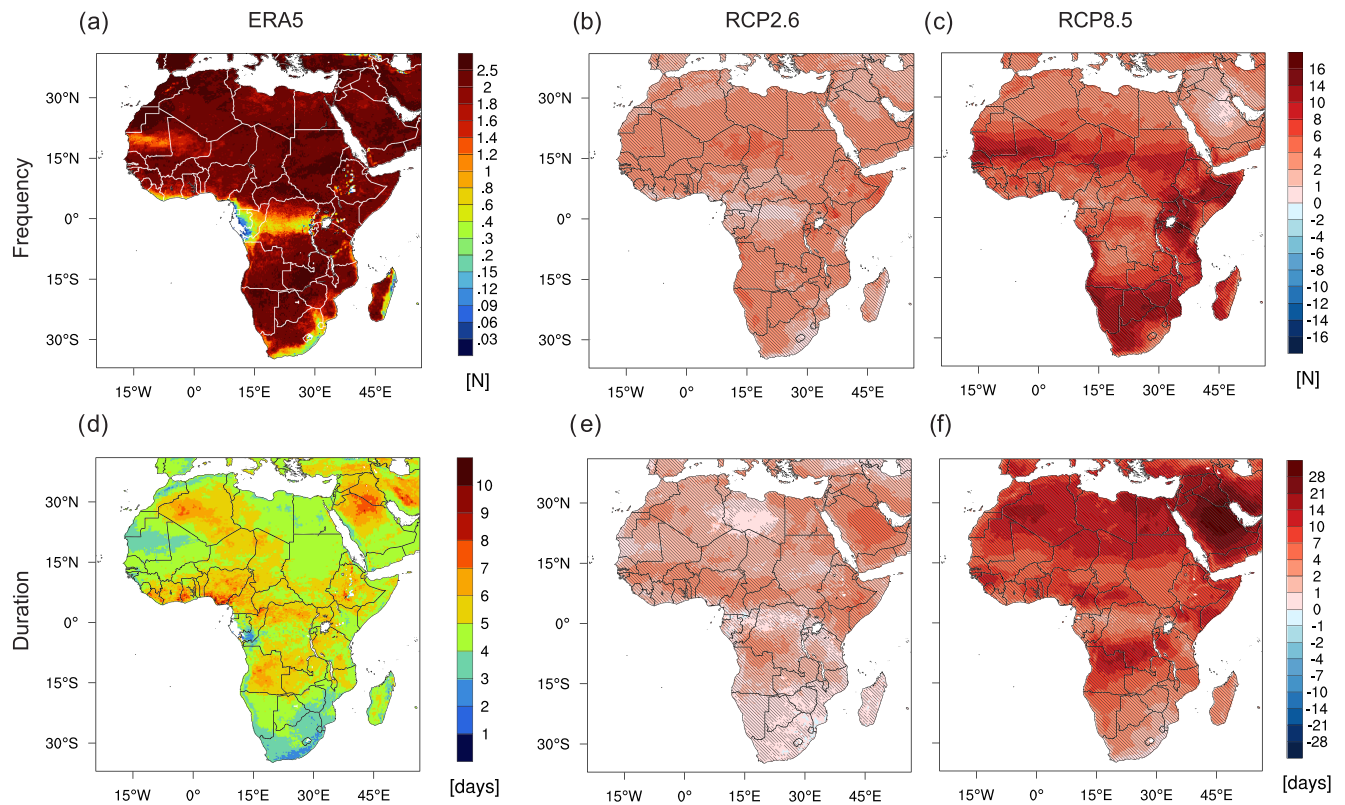


Figure 1. (a) Mean annual frequency and (d) mean duration of coincident heat waves and droughts calculated from the ERA5 data set for the reference period 1981–2010. Projected changes of annual frequency and duration of coincident heat waves and droughts as ensemble mean using (b, e) RCP2.6 and (c, f) RCP8.5 for the scenario period 2070–2099/1981–2010. The hatched areas indicate high model agreement ($n \geq 4$) of the sign of the climate change signal.

3.1.2. Heat Waves and Extreme Precipitation

This compound event occurs notably less frequently than coincident heat waves and droughts with on average 0.03 to 0.6 incidences per year in the reference period, which is limited by the infrequent occurrence of extreme precipitation (Figure 2a). It appears only in West and Central equatorial Africa, coastal regions of East and Southeast Africa, and East Madagascar. In the RCP2.6 scenario, an increase in frequency is projected of about 0.1 to 0.6 events per year over Equatorial Guinea and Gabon, and of about 0.1 to 0.2 events per year over Southeast Africa and East Madagascar with high model agreement (Figure 2b). In the RCP8.5 scenario, this event appears in all sub-Saharan regions. A distinct increase is projected for West-Central Africa, the mountainous regions of Ethiopia, East to Southeast Africa, and Madagascar accompanied by high model agreement (Figure 2c). The strongest increase in frequency with up to six events per year is shown for West-Central Africa. The coincident appearance of heat waves and extreme precipitation lasts about 1.5 days for today's climate (Figure 2d) and shows only a small increase in duration by up to 0.5 days over Gabon and Madagascar for both scenarios (Figures 2e and 2f).

3.2. Sequential Climate Extremes

3.2.1. Droughts and Extreme Precipitation

Almost the entire African continent is affected by sequential droughts and extreme precipitation events with different annual frequencies in the reference period. The highest frequencies appear with 1 to 2.5 events per year and more in Morocco, Northern Algeria, along the coast of the Mediterranean Sea, East Africa, and Southern Africa, and the lowest ones along coastal areas of West and West-Central Africa (Figure 3a). For the RCP2.6 scenario, the models project small changes of between -0.4 and 0.6 events per year with mostly high model agreement (Figure 3b). The climate change signal becomes clearer for the entire continent under RCP8.5 showing an increase in frequency of about 0.2 to 2 events per year for regions between 15°S and 15°N , Madagascar and eastern South Africa (Figure 3c). A decrease in frequency of between -0.6 and 0 events

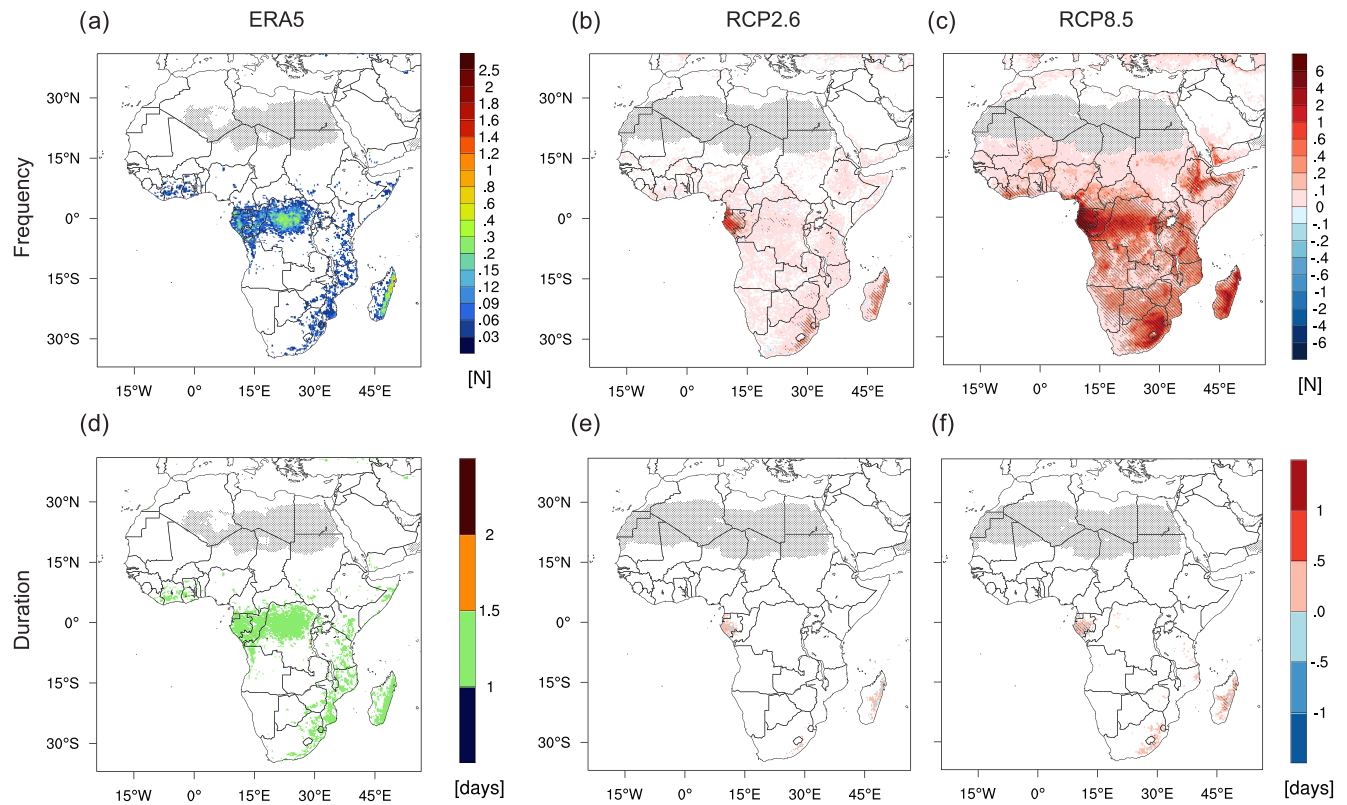


Figure 2. (a) Mean annual frequency and (d) mean duration of coincident heat waves and extreme precipitation calculated from the ERA5 data set for the reference period 1981–2010. Projected changes of annual frequency and duration of coincident heat waves and extreme precipitation as ensemble mean using (b, e) RCP2.6 and (c, f) RCP8.5 for the scenario period 2070–2099/1981–2010. The dotted areas denote not sufficient ($n < 100$) wet days in 30 years to determine the 95th percentile precipitation, and the hatched areas indicate high model agreement ($n \geq 4$) of the sign of the climate change signal.

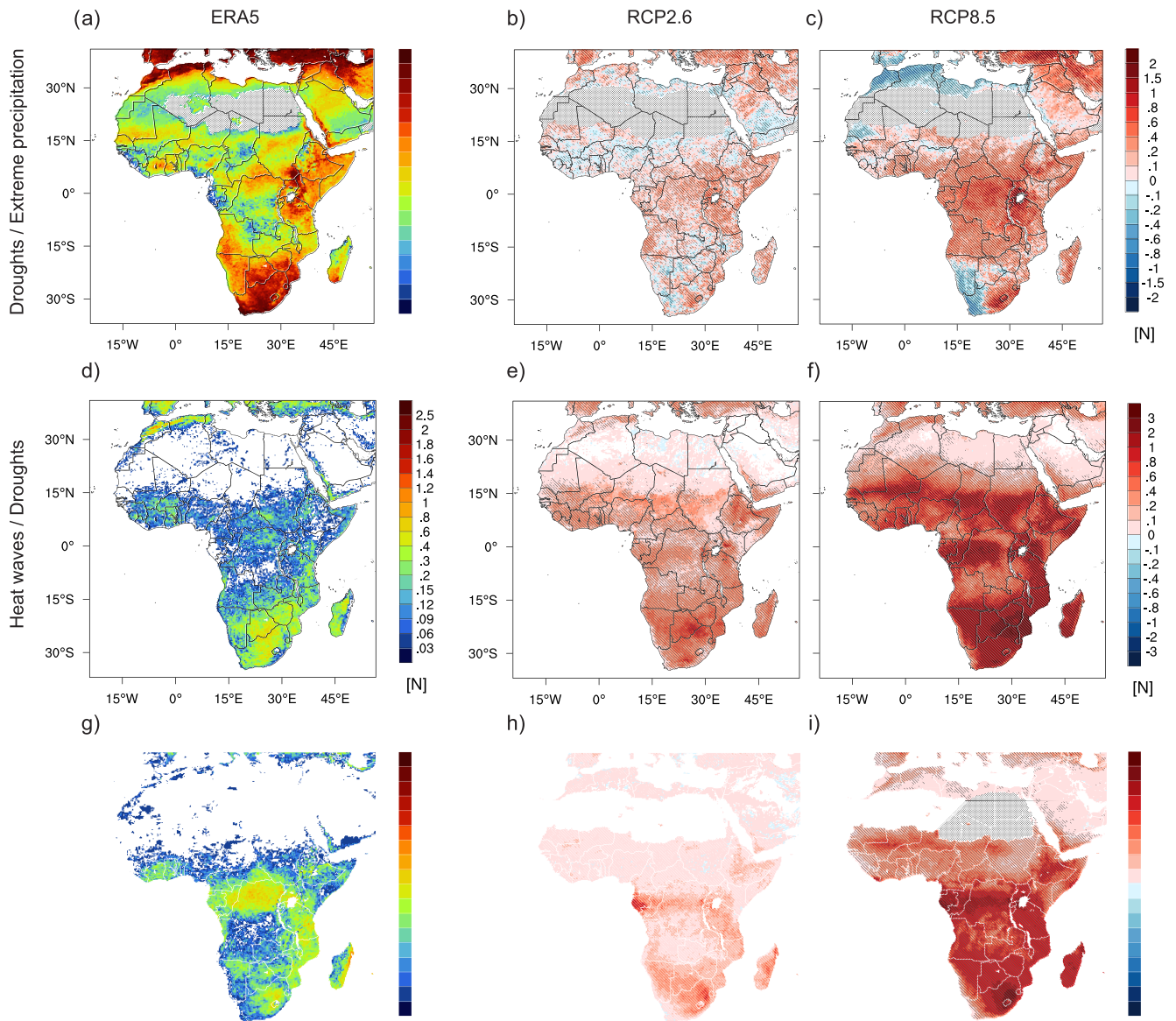
per year is projected for North Africa and Southwest Africa. This is caused by less frequent single events of droughts and extreme precipitation in these regions (not shown). All distinct changes in frequency show high model agreement in RCP8.5.

3.2.2. Heat Waves and Droughts

In the present climate, sequential heat waves and droughts appear in Morocco, Northern Algeria, and in sub-Saharan Africa, but not in the Sahara (Figure 3d). This is explained by the fact that heat waves and droughts occur mainly coincidentally and not sequentially in the desert. Highest frequencies of sequential heat wave and drought events can be observed with values from 0.2 to 0.8 events per year in Northern Algeria, Southern Africa, Madagascar, and up to one event per year in Morocco. Both scenarios show more frequent events in the future with increases of 0.1 to 1 events per year for RCP2.6 and with 0.4 to 3 more events per year for RCP8.5 in sub-Saharan Africa (Figures 3e and 3f). The most affected regions are along or south of 15°N, along the Equator, Southern Africa, and Madagascar with high model agreement. The climate change pattern of RCP8.5 seems to be dominated by the climate change signal of heat waves as analyzed under 2°C and 3°C global warming by Weber et al. (2018).

3.2.3. Heat Waves and Extreme Precipitation

Under present climate conditions, sequential heat waves, and extreme precipitation events occur mostly in sub-Saharan Africa, in particular with high frequencies of 0.3 to 1.2 incidences per year in Central Africa, East to Southeast Africa, and East Madagascar (Figure 3g). In the RCP2.6 scenario, the models simulate an increase of sequential events of 0.2 to 0.6 events per year for equatorial and Southern Africa, Madagascar, and of up to one event per year in Gabon (Figure 3h). A distinct increase of sequential heat waves and extreme precipitation is simulated in the RCP8.5 scenario for the whole of sub-Saharan Africa (Figure 3i). The strongest increase is projected with one to four more events per year at the equator,



Ethiopia, Tanzania, and Southern Africa (except for southwestern parts) including Madagascar. In both scenarios, the frequency increase is accompanied by high model agreement.

3.3. Exposed Population

3.3.1. Projected African Population Growth

In the population reference period (1981–2005) areas of largest population are located in North Africa in Morocco, North Algeria, and along the Nile and its delta, in West Africa along the coastal regions of the Gulf of Guinea and Nigeria, in East Africa in Ethiopia and around the Lake Victoria, and Southeast Africa (Figure 4a). For the end of the century the SSP1 scenario projects noticeable population growth along the coastal regions from Morocco to Libya, between 15°S and 15°N, Southeast Africa and Madagascar

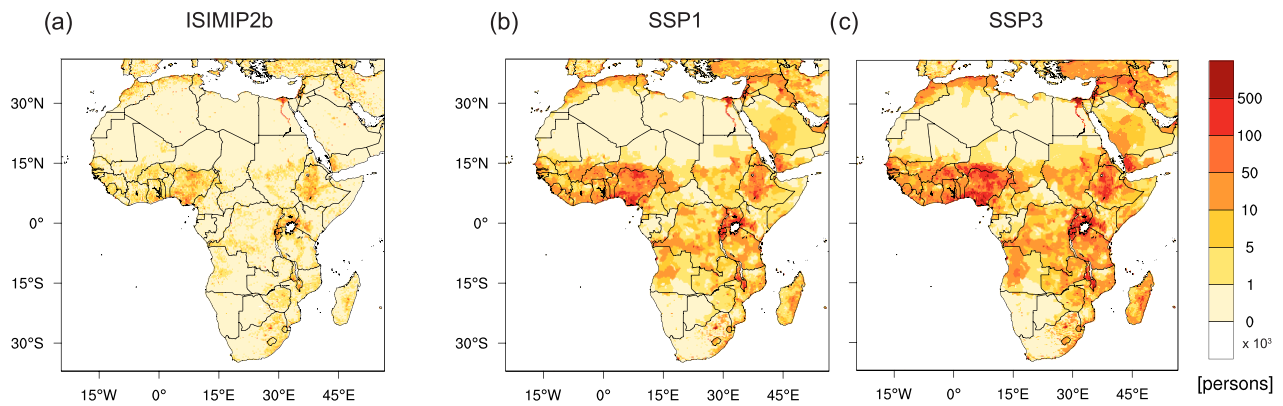


Figure 4. (a) Mean population derived from ISIMIP2b for 1981–2005 and from (b) SSP1 and (c) SSP3 for 2070–2100.

(Figure 4b). Strong population growth is expected along the Nile and its delta, Nigeria, Ethiopia, around Lake Victoria and Malawi. This trend is projected to intensify in the SSP3 scenario (Figure 4c).

3.3.2. Exposure to Coincident Heat Waves and Droughts

Mean annual exposure to coincident heat waves and droughts amounts to between 0 and 5,000 person-events per grid box for uppermost North and sub-Saharan Africa for the reference period, but with higher exposure between 5,000 and 500,000 person-events in populous regions along the coastal regions from Morocco to North Tunisia, West Africa, Ethiopia, around Lake Victoria, and Malawi. However, the exposure exceeds 500,000 person-events in the Nile Delta (Figure 5a).

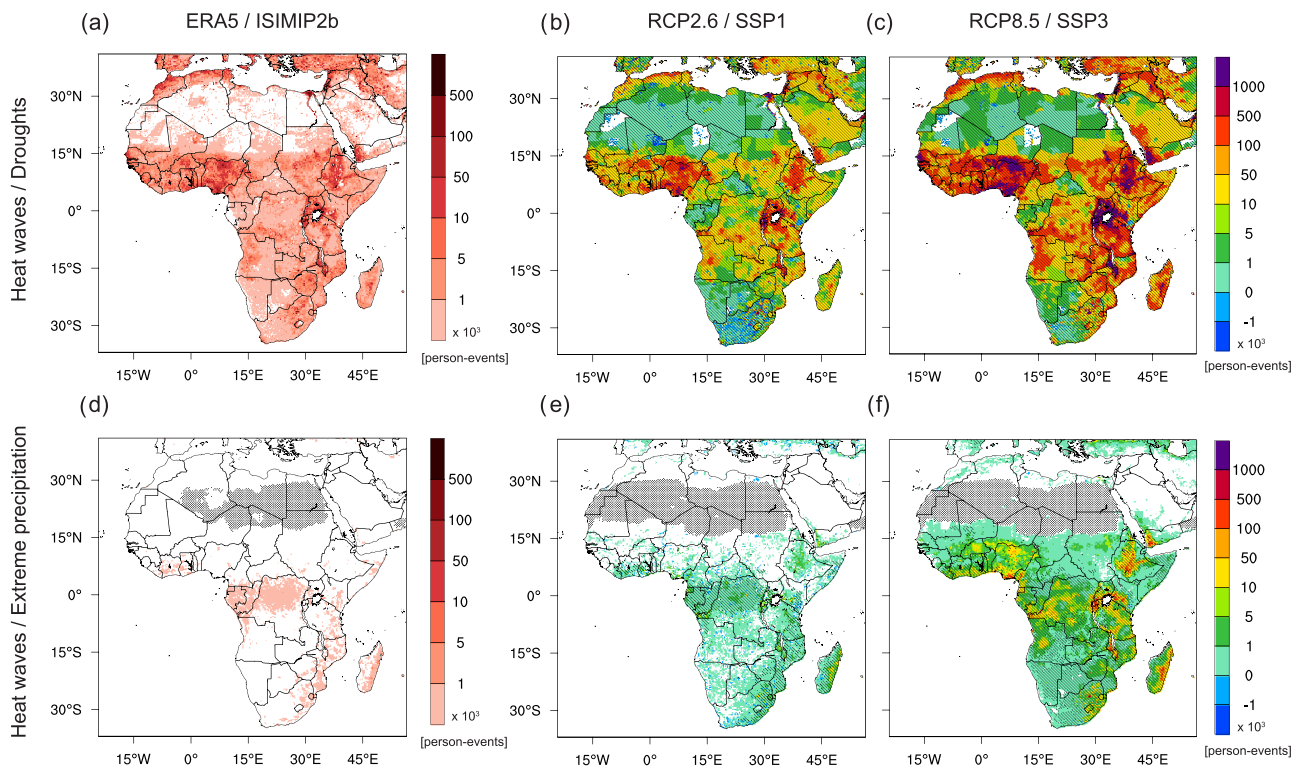


Figure 5. (a, d) Exposure to coincident climate extremes calculated from the ERA5 and the ISIMIP2b population data set for the reference period 1981–2010. Projected changes in exposure to coincident climate extremes as ensemble mean using (b, e) RCP2.6/SSP1 and (c, f) RCP8.5/SSP3 for the scenario period 2070–2099/1981–2010. The dotted areas denote not sufficient ($n < 100$) wet days in 30 years to determine the 95th percentile precipitation, and the hatched areas indicate high model agreement ($n \geq 4$) of the sign of the climate change signal.

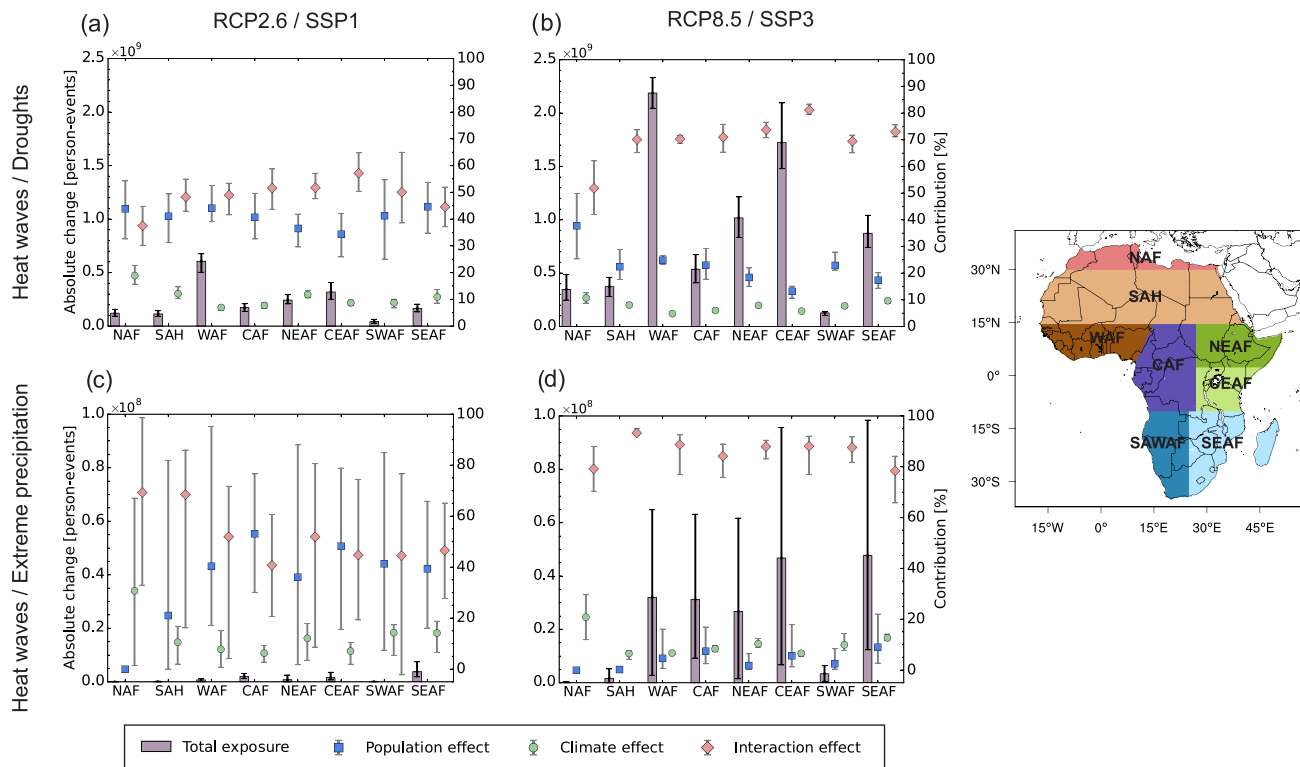


Figure 6. Regional sums of change in exposure to coincident climate extremes for different African subregions (bars, primary y axis) and relative contribution of the population, climate, and interaction effects (marker, secondary y axis). (a, c) RCP2.6/SSP1 and (b, d) RCP8.5/SSP3 for scenario period 2070–2099/1981–2010. The whiskers show the ensemble minimum and maximum. The African subregions are denoted as Sahara (SAH), West Africa (WAF), Central Africa (CAF), Northeast Africa (NEAF), Central-East Africa (CEAF), Southwest Africa (SWAF), Southeast Africa (SEAF), and North Africa (NAF).

At the end of the century, the exposure increases in the aforementioned regions and expands in the same areas for RCP2.6/SSP1 with high model agreement (Figure 5b). For the RCP2.6/SSP1 scenario, the strongest growth in mean exposure is projected for WAF (605.8 million person-events), CEAF (318.5 million person-events), and NEAF (242.7 million person-events) for RCP2.6/SSP1 (Figure 6a; Table S1). In this scenario, the interaction effect (as a product of population growth and increase in frequency of compound events) contributes with up to 57.1% in six out of eight subregions at most (except for NAF and SEAF) to the exposure change (Table S2). In the RCP8.5/SSP3 scenario, the exposure increases strongly for almost all regions between 15°S and 15°N as well as Southeast Africa and Madagascar showing high model agreement (Figure 5c). The strongest growth in mean exposure is simulated for WAF (2.2 billion person-events), CEAF (1.7 billion person-events), and NEAF (1.0 billion person-events) (Figure 6b; Table S3), whereas the interaction effect makes up the most contributions from 51.8% to 81.1% to the exposure change in RCP8.5/SSP3 (Table S4).

3.3.3. Exposure to Coincident Heat Waves and Extreme Precipitation

In the reference period, the exposure by annual coincident heat waves and extreme precipitation stretches over West and Central equatorial Africa, small areas from East to Southeast Africa and East Madagascar with values between 0 and 1,000 person-events per grid box (Figure 5d).

For RCP2.6/SSP1 scenario the model ensemble projects mainly a growth in exposure for sub-Saharan Africa including Madagascar, especially in the aforementioned regions with high model agreement (Figure 5e). The three regions with the highest change in mean exposure are SEAF (3.8 million person-events), CAF (1.9 million person-events), and CEAF (1.5 million person-events) (Figure 6c; Table S5). In six out of eight subregions, the interaction effect contributes to the exposure change with a maximum of 69.3% (Table S6). The broad bandwidths of relative contribution effects are caused by the high variability in the model results. In the RCP8.5/SSP3 scenario, the exposure increases and covers the coastal regions of West

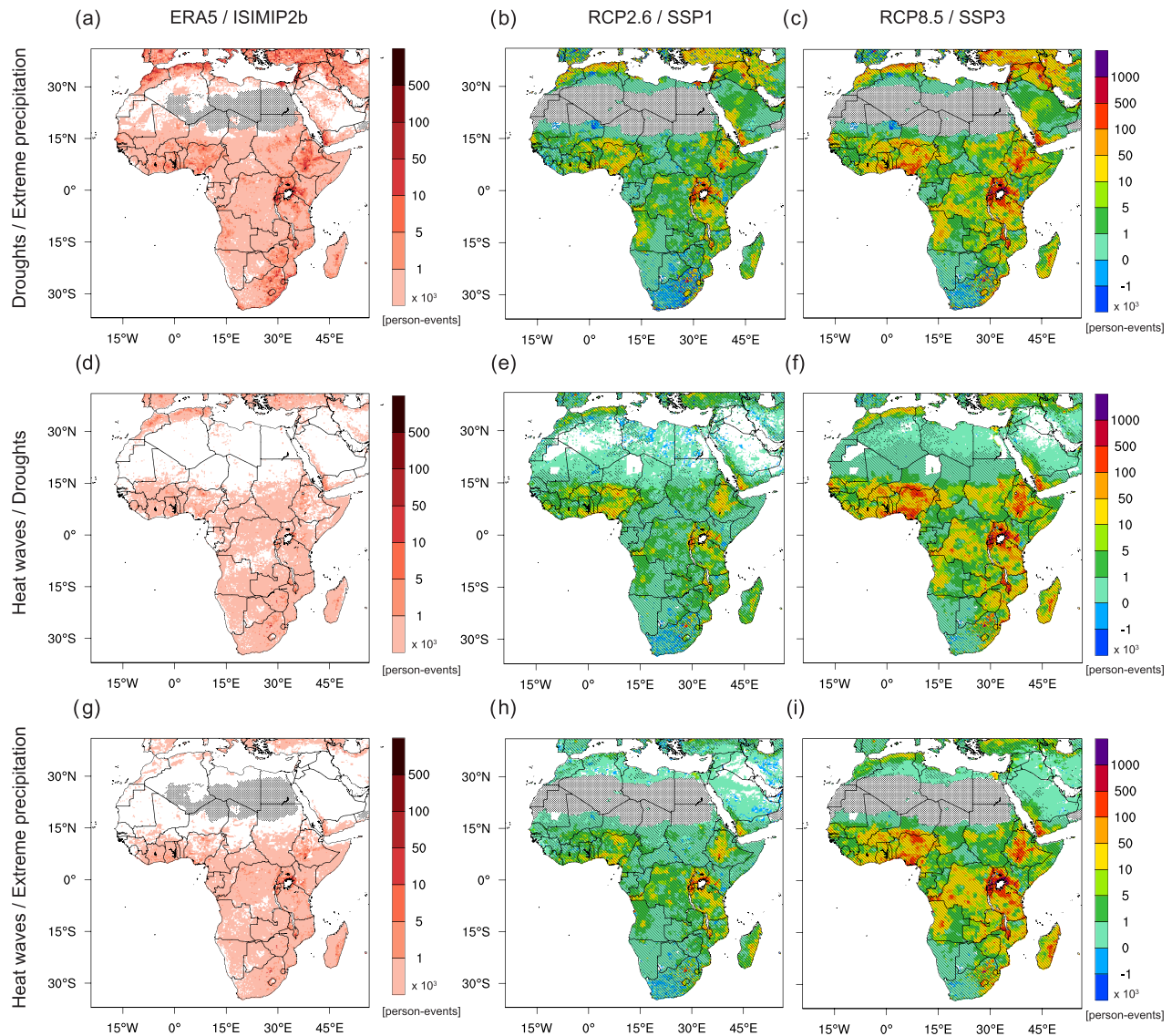


Figure 7. (a, d, and g) Exposure to sequential climate extremes calculated from the ERA5 and the ISIMIP2b population data set for the reference period 1981–2010. Projected changes in exposure to sequential climate extremes as ensemble mean using (b, e, and h) RCP2.6/SSP1 and (c, f, and i) RCP8.5/SSP3 for the scenario period 2070–2099/1981–2010. The dotted areas denote not sufficient ($n < 100$) wet days in 30 years to determine the 95th percentile precipitation, and the hatched areas indicate high model agreement ($n \geq 4$) of the sign of the climate change signal.

Africa, Ethiopia, from the Equator to South Africa, and Madagascar with high model agreement (Figure 5f). In detail, the highest increase in mean exposure is simulated for SEAF (47.7 million person-events), CEAF (46.8 million person-events), and WAF (32.0 million person-events) (Figure 6d; Table S7). However, the growth in exposure coincides with a high uncertainty depicted by broad bandwidths that may be caused by the high spatial variability of the extreme precipitation component. Major relative contributor to the exposure change is the interaction effect with a range between 78.4% and 93.3% in the different subregions (Table S8).

3.3.4. Exposure to Sequential Droughts and Extreme Precipitation

For present climate conditions, almost the entire African continent, except the Sahara, exhibits an exposure to annual sequential droughts and extreme precipitation with values between 0 and 1,000 person-events per grid box and higher exposure between 5,000 and 100,000 person-events along the coastal regions from Morocco to North Tunisia, in the Nile Delta, West Africa, Ethiopia, around Lake Victoria, and Southeastern Africa (Figure 7a).

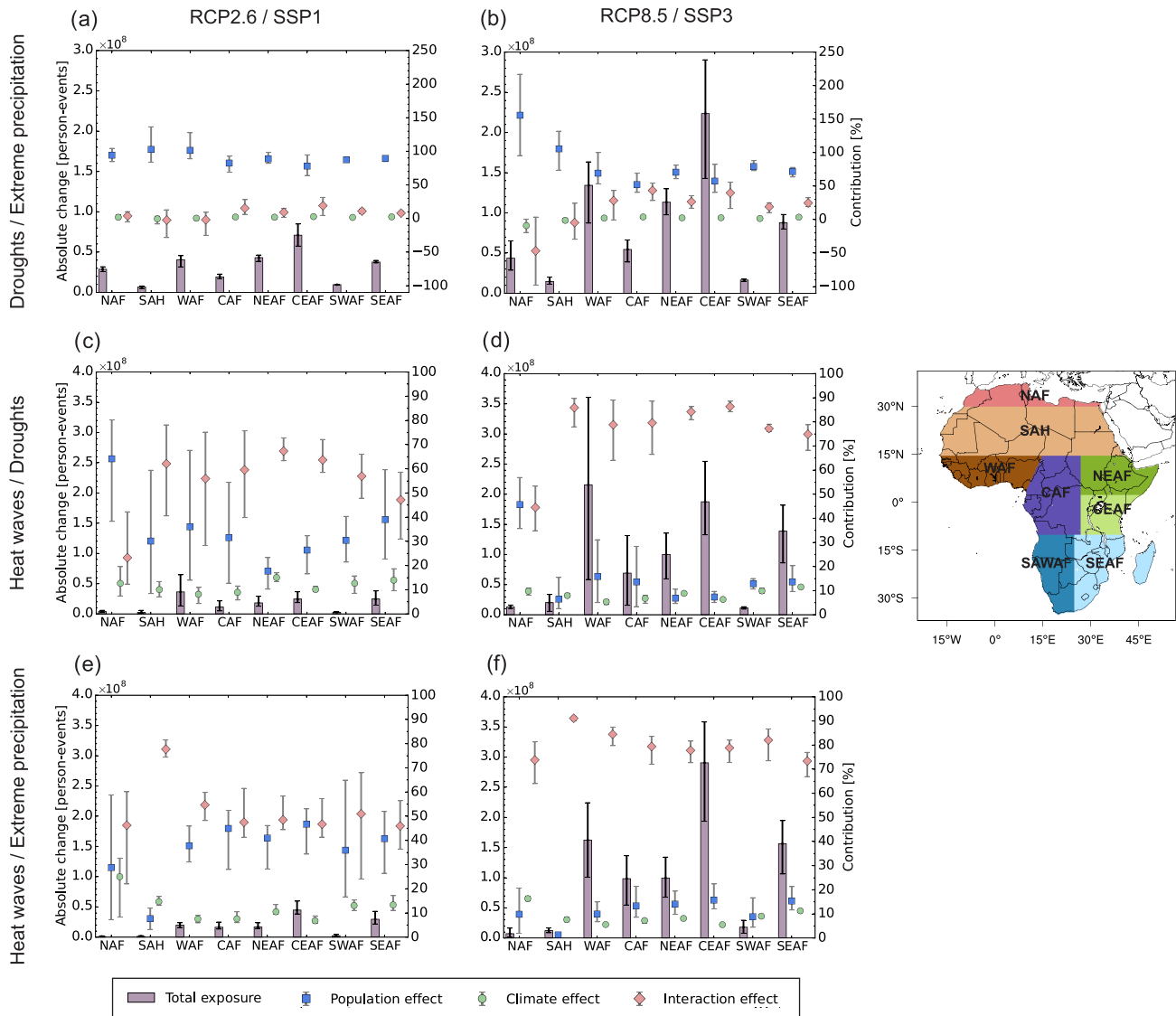


Figure 8. Regional sums of change in exposure to sequential climate extremes for different African subregions (bars, primary y axis) and relative contribution of the population, climate, and interaction effects (marker, secondary y axis). (a, c, and e) RCP2.6/SSP1 and (b, d, and f) RCP8.5/SSP3 for scenario period 2070–2099/1981–2010. The whiskers show the ensemble minimum and maximum. The African subregions are denoted as Sahara (SAH), West Africa (WAF), Central Africa (CAF), Northeast Africa (NEAF), Central-East Africa (CEAF), Southwest Africa (SWAF), Southeast Africa (SEAF), and North Africa (NAF).

In the RCP2.6/SSP1 scenario, the exposure increases particularly in the aforementioned regions and expands in some areas in sub-Saharan Africa, but decreases in South Africa except for the eastern coastal regions (Figure 7b). The projected changes show high model agreement for the entire continent. The regions with the highest growth in mean exposure are CEAF (71.0 million person-events), NEAF (43.1 million person-events), and WAF (40.6 million person-events), whereas the population effect accounts for 78.1% to 102.8% of the exposure change in the different subregions (Figure 8a; Tables S9 and S10). Values of more than 100% are a result of high absolute values of the population effect and lower absolute values of exposure change caused by negative absolute values of the climate and interaction effect. In the RCP8.5/SSP3 scenario, the trend of increasing exposure by annual sequential events strengthens for the whole of Africa and results in more positive exposure change in eastern parts of South Africa with high model agreement (Figure 7c). In detail, the regions with the strongest growth in mean exposure are CEAF (223.6 million person-events), WAF (134.3 million person-events), and NEAF (113.3 million person-events) (Table S11). Similar to the RCP2.6/SSP1 scenario, the population effect contributes most to the absolute change in

exposure with a range between 52.5% and 155.8% in the different subregions (Figure 8b; Table S12). Due to the fact that sequential droughts and heat waves are projected to be less frequent in NAF and SAH (see Figure 3c), the climate contribution to the exposure change is negative and caused a negative interaction effect in these subregions.

3.3.5. Exposure to Sequential Heat Waves and Droughts

Exposure to sequential heat waves and droughts is given in the uppermost North Africa and sub-Saharan Africa between 0 and 1,000 person-events in the reference period. Higher exposure between 1,000 and 10,000 person-events is located in isolated areas of Morocco and North Algeria, Nigeria, around Lake Victoria, and Southern Africa (Figure 7d).

Under the RCP2.6/SSP1 scenario, the exposure increases over the entire African continent, except for South Africa, showing a decrease for most areas, which coincides with high model agreement (Figure 7e). A clear increase in exposure is projected for North Algeria, West Africa and Ethiopia, around Lake Victoria, and Malawi. The highest values of mean exposure are simulated for WAF (36.4 million person-events), SEAF (24.6 million person-events), and CEAF (24.5 million person-events) (Table S13). The interaction effect contributes up to 67.3% at most to the exposure change, except for NAF, where the population effect is higher (Figure 8c; Table S14). Under the RCP8.5/SSP3 scenario, a strong increase in exposure is simulated for African regions between 15°S and 15°N including Madagascar with high model agreement (Figure 7f). The subregions showing the highest increase in mean exposure are WAF (215.6 million person-events), CEAF (187.4 million person-events), and SEAF (138.7 million person-events), but the values have an inherent uncertainty depicted through broad bandwidths (Table S15). The interaction effect contributes up to 86.3% at most to the growth in exposure change, except for NAF, where the contribution of the population effect is higher (Figure 8d; Table S16).

3.3.6. Exposure to Sequential Heat Wave and Extreme Precipitation

In the present climate, the population in sub-Saharan Africa and Madagascar is mainly subjected to exposure by sequential heat waves and extreme precipitation up to 1,000 person-events per grid box (Figure 7g). A higher exposure is observed between 5,000 and 50,000 person-events in Ethiopia, around Lake Victoria, and Malawi.

The RCP2.6/SSP1 scenario shows an increase in exposure in West Africa, Ethiopia, Central Africa, around Lake Victoria, East to Southeast Africa, and East Madagascar (Figure 7h). A decrease in exposure is simulated for western South Africa. All changes in exposure exhibit high model agreement. The highest increase in mean exposure is simulated for CEAF (44.8 million person-events), SEAF (29.6 million person-events), and WAF (19.8 million person-events) (Table S17). The interaction effect contributes with 46.0% to 77.7% in seven out of eight subregions at most to the exposure change, except for CEAF where the population and interaction effects are equal (Figure 8e; Table S18). In the RCP8.5/SSP3 scenario, the increase in exposure expands in area from Morocco to North Tunisia and the Nile Delta, sub-Saharan Africa, and Madagascar, except for Namibia, Botswana, and western South Africa, which show mainly a small increase in exposure (Figure 7i). A strong growth in exposure is projected for Nigeria, Ethiopia, around Lake Victoria, and Malawi. The increase in exposure coincides with high model agreement. The subregions showing the highest increase in exposure are CEAF (290.6 million person-events), WAF (162.5 million person-events), and SEAF (156.4 million person-events) (Table S19). The largest contributor to the growth in the exposure change is the interaction effect with a range from 73.4% to 91.1% (Figure 8f; Table S20).

4. Discussion

This work has analyzed changes in a range of different compound events over Africa, both in terms of their overall incidence, but also combined with projected changes in population to provide estimates of the number of people exposed to such events at the end of the century (2070–2099). The results clearly show that for all of the compound events analyzed, some considerable changes will be seen over large parts of Africa by the end of the century, with the changes in the incidence of such events being greater under the higher emissions RCP8.5 scenario compared to RCP2.6. Understanding the causal factors that would explain these projected changes in compound events goes beyond the scope of this paper. Nevertheless, it is possible to suggest possible mechanisms that could explain these patterns. For example, changes in large-scale circulation (including the movement of the Inter Tropical Convergence Zone [ITCZ]), sea surface temperature,

insulation, soil moisture, and related processes could all play a part in helping to explain the changes in heat waves, droughts, and extreme precipitation that compose the compound events that we have analyzed here. This is clearly an issue requiring further research and analysis.

The most significant compound event over Africa in terms of the number of people exposed is coincident heat waves and drought (Tables S21–S23). This is true for both the RCP2.6/SSP1 and RCP8.5/SSP3 scenarios, with the multimodel mean projection showing there to be ~1.9 billion and ~7.3 billion person-events, respectively, across the African continent. These numbers represent a 14- and 52-fold increase in the number of person-events compared to the reference period. The least significant compound event in terms of the number of people exposed is coincident heat waves and extreme precipitation, with the multimodel mean projection showing there to be ~9.4 million and ~190 million person-events under RCP2.6/SSP1 and RCP8.5/SSP3 scenarios, respectively, which represents a 17- and 342-fold increase compared to the reference period (Tables S22 and S23). Clearly, while coincident heat waves and extreme precipitation are the least important in absolute terms, they are the most important in terms of relative change, certainly under RCP8.5/SSP3 (Table S23). As such, this compound event may represent an emerging threat in Africa, which, given that the awareness of this compound event will most likely be low, could present a particular challenge in planning to adapt for it. For the other compound events, there are generally relatively small differences between them in terms of the number of person-events (Tables S21–S23).

Within Africa, different regions are more exposed than others to the different compound events. Overall, however, irrespective of whether or not the compound events are considered individually or in aggregate, there are four regions that consistently appear to be particularly exposed. These are West Africa, Central-East Africa, Northeast Africa, and Southeast Africa (Tables S21–S23). This pattern is consistent across both RCP2.6/SSP1 and RCP8.5/SSP3 scenarios. That West Africa and central and eastern parts of Africa are shown to have the largest exposed populations (in both absolute and relative terms) to these compound events provides further evidence that these areas are particularly at risk from climate change. This finding supports the research of Ahmadalipour et al. (2019), Rohat et al. (2019), and Russo et al. (2019), who, while analyzing different climate risks, all showed that these same regions would be particularly exposed in the future. It is also worth noting that in terms of the overall ranking of regions based on an aggregation of person-events across the five compound events, that North Africa falls down the ranking the most, going from rank two in the reference period, to rank six (based on absolute numbers), and rank eight (based on relative change in the number of person-events) by the end of the century, and this is true across both scenarios (cf. Tables S21–S23). West Africa is the most exposed region overall, in absolute terms by the end of the century, but in terms of the relative increase, Central-East Africa is the most exposed region. This is a finding that Rohat et al. (2019) also made in their analysis of changes in exposure to dangerous heat in African cities. This pattern of most (and least) exposed regions is largely explained by differences in population growth over the 21st century, with western and eastern African countries generally projected to grow more rapidly than North African countries. This point is clearly of importance when considering an appropriate policy response to address these climate risks, particularly for regional development banks and agencies (Muccione et al., 2016).

Understanding the relative importance of the different drivers of the change in the projected exposure to the different compound events (climate, population, and interaction effects) provides an important means of informing a policy response to try and reduce the exposure of the African population.

For both coincident compound events, under the RCP2.6/SSP1 scenario the interaction and population effects explain most of the change in exposure, with the interaction effect generally being dominant across all regions (Figure 6). Under the RCP8.5/SSP3 scenario, the interaction effect is completely dominant in explaining the change in exposure to both compound events. In both scenarios and for all coincident compound events, the climate effect alone is shown to play a minor role in explaining the change in exposure.

For the sequential droughts and extreme precipitation, the population effect is the dominant factor in explaining change in exposure, and this is true across both scenarios, with the importance of the interaction effect increasing somewhat under the RCP8.5/SSP3 scenario (Figures 8a and 8b). The climate effect is shown to be of minor importance. For the sequential heat waves and droughts, the interaction effect is the dominant factor in explaining change in exposure in all regions apart from North Africa, and across both scenarios (Figures 8c and 8d). The climate effect alone is again shown to be of minor importance. For sequential

heat waves and extreme precipitation, the population and interaction effects are the most important in explaining change in exposure, with the interaction effect being dominant, and this dominance is particularly marked under RCP8.5/SSP3 (Figures 8e and 8f). The climate effect is again shown to be of minor importance in explaining the change in exposure.

Taken together, these results show that generally, across all compound events and scenarios, the change in exposure at the end of the 21st century is explained mostly by the interaction effect, and population effect, with the climate effect playing a very minor role overall. Placing these results in the context of the broader literature on changes in exposure to climate risks is not straightforward, since to date there are no comparable studies for Africa in relation to compound events. This limitation notwithstanding, it is still possible to make some broad comparisons. The dominance of the interaction effect found here is broadly in keeping with the findings of Liu et al. (2017) in their analysis of changes in exposure to extreme heat, but in our analysis, the importance of the population effect is much greater than the climate effect, which is different from what Liu et al. report for Africa. Our results are also similar to those of Rohat et al. (2019), who report that by the end of the 21st century, the most important drivers of change in the regions of Africa that they analyzed were the interaction effect and population effect and that the climate effect alone was generally not that important in explaining changes in exposure. That the climate effect plays such an unimportant role in the results presented here differs from the findings of Coffel et al. (2018), who in their global analysis of exposure to heat stress found that the climate effect was the most important driver in exposure; however, they also reported that in hot regions (Africa being one), the interaction effect was a considerable factor. That the climate effect is of minor importance in driving changes in exposure in our analysis is due to the fact that we are analyzing changes in two climate events, which, in purely probabilistic terms, reduces the size of the projected changes that we are likely to see. In contrast to similar analyses focusing on changes in exposure to one climate hazard, the changes that we report in the incidence of compound events are thus relatively modest. However, while changes in the frequency of compound climate events may not individually be the main driver of changes in exposed population, the influence of climate change is expressed strongly through the interaction effect with rapid population growth in Africa by the end of the 21st century.

Given the importance of the interaction and population effects, clearly, any policy response designed to reduce the exposure of African populations to these compound events needs to focus on both regional socioeconomic development (and thus population growth) and climate mitigation efforts. The importance of the focus of the policy response on these two factors is underscored by analysis of the difference in exposure under the two different scenarios we investigated. Aggregating across compound events, under RCP2.6/SSP1 (stringent mitigation and slow population growth), the increase in exposure compared to the present-day for Africa as a whole is ~2.3 billion person-events, which compares to an increase of ~9.7 billion person-events under a worst-case climate scenario RCP8.5, together with fast population growth (SSP3) (Tables S22 and S23). These figures represent a 12- and 47-fold increase in exposure compared to the present-day. Clearly, being able to achieve rapid and major reductions in global carbon emissions, together with faster socioeconomic and regional development in Africa, would lead to a huge reduction in exposure of ~7.4 billion person-events. This much-reduced exposure under RCP2.6/SSP1 compared to RCP8.5/SSP3 is, as to be expected, true across all individual compound events (Tables S22 and S23). While it is clearly the case that the RCP2.6/SSP1 scenario is much more desirable than the RCP8.5/SSP3 scenario, realizing this highly ambitious scenario is nevertheless still projected to result in a 6- to 17-fold increase in the absolute exposure when aggregating all compound events, compared to the present-day, across all regions. As such, this would still represent a major adaptation challenge, requiring an effective policy response (Hoegh-Guldberg et al., 2019).

While our analysis identifies West Africa and eastern and central regions of Africa as being particularly exposed to changes in the compound events we have investigated, it necessarily provides an incomplete picture of the full policy response, and priorities that may be set, as our analysis provides no information in relation to the vulnerability and adaptive capacity of these different areas (Williges et al., 2017). Our analysis provides changes at a relatively high spatial resolution of 28 km. Ideally, we would be able to combine this information on changes in compound event hazard and population exposed with similar gridded information in relation to a range of socioeconomic and sociopolitical factors, which are typically used as indicators of vulnerability and adaptive capacity (Thomas et al., 2018). Sadly, this is not possible today, since such data

sets do not exist for Africa, and indeed many other parts of the world (Stern et al., 2013). The analyses that do consider changes in vulnerability and adaptive capacity in Africa, have all been at the national level where the necessary data sets are more readily available (Ahmadalipour et al., 2019; Asefi-Najafabady et al., 2018). We did not consider this a useful addition to this analysis at this point but clearly appropriate consideration needs to be given to these issues when developing a policy response.

Our analysis has shown that there are major projected increases in the exposure of the African population to a range of different compound events. It is however important to address some limitations in relation to the sensitivity of the results to changes in the way in which the climate hazards are defined. Clearly, if the results of our analysis were overly sensitive to the way in which the hazards were defined, then our interpretation of the results and conclusions may be affected. To investigate this issue, we carried out a sensitivity analysis in relation to the number of dry days required in order to trigger a drought event, when analyzing the sequential droughts and extreme precipitation. Figure S2 shows the results of varying the number of dry days from three to five, and to seven. Clearly, there is a negative relationship between the number of dry days and the incidence of this compound event. While the quantity of such events clearly changes, the overall qualitative spatial pattern of the changes does not change, with the same areas being affected. As such, any policy response informed by these results would still focus on the same areas regardless of how the drought length was specified. We take this as an indication of a robust finding for sequential droughts and extreme precipitation in the analysis that we present.

An additional limitation is that, while we have made use of the best currently available regionally down-scaled climate projection data set from CORDEX-CORE, the ensemble size is small. The applied model ensemble comprises only five ESM/RCM members in which only three Earth System Models (ESM) and two Regional Climate Models (RCMs) are used, within which the regional climate model REMO is over-represented, composing as it does three of the five RCM combinations. As such, our analysis, while based on the best currently available high-resolution climate and population data for Africa, provides a necessarily limited quantification of uncertainty in the projected changes in compound events. Moreover, both RCMs utilize parameterized convection schemes, that is, no resolved convection, and as such, it is to be expected that different results might be obtained with convection permitting models (Kendon et al., 2019).

5. Conclusions

Knowledge of the incidence of, and exposure of the African population to, compound climate events is currently very poor. This paper has analyzed projected changes in the incidence of five different compound events, and the exposure of the African population to them at the end of the 21st century, for two different scenarios, one based on an assumption of stringent reductions in global carbon emissions, and rapid socio-economic development (RCP2.6/SSP1), and the other based on continued growth in global carbon emissions together with slow socioeconomic development (RCP8.5/SSP3). We show that the incidence of all compound events will increase by the end of the century under both scenarios, which, when combined with projections of population change and aggregated across all compound events, results in a projected 12- to 47-fold increase in exposure compared to the present-day, under RCP2.6/SSP1 and RCP8.5/SSP3, respectively. The difference between these two different possible future worlds translates into a reduction of ~7.4 billion person-events in the RCP2.6/SSP1 scenario. This is further evidence of, and motivation for, the need to urgently and massively reduce global carbon emissions and reach net-zero emissions as soon as possible.

The regional pattern of exposure to these compound events with West Africa, Central-East Africa, Northeast Africa, and Southeast Africa, being the four regions with the largest exposure at the end of the 21st century, is of significance for regional development and potentially also in relation to climate finance decision making. However, because our analysis only focuses on changes in exposure at the end of the 21st century, we have presented no evidence of how quickly the ranking of the different subregions may change over time. In our analysis we show that at the end of the century, Central-East Africa rises to being the second most exposed region, compared to the fifth most exposed region in the present-day. Similarly, North Africa falls from being the second most exposed region in the present-day to the sixth most important at the end of the century. Clearly, development and investment decisions are made for a range of time horizons, and as such, being able to understand the temporal evolution of exposure in the different regions would represent a valuable piece of information. This is an avenue of future work that is worthy of exploration. This

exploration of the temporal evolution of exposure should of course be coupled with analysis of the drivers of change. We have shown that overall the interaction effect (simultaneous changes in population and climate change) and the population effect are the main drivers of changes in exposure at the end of the century, but how the importance of these drivers change through time may provide important insights for the development of effective adaptation responses.

Taken together, these insights highlight the need for careful analysis of these results in order to inform and develop effective policy responses, which will require not only strong mitigation action at the global level, but also rapid socioeconomic development at the regional level, in order to reduce the exposure of the African population. Even if such mitigation and development policies were successful in realizing something like an RCP2.6/SSP1 scenario, this would still represent a considerable adaptation challenge, and effective adaptation policies would need to be developed to deal with the still major projected increases in exposure in such a world, by the end of the 21st century.

Being able to connect the incidence of these compound events with direct societal impacts is an area in need of major new research in general, and for the African continent in particular. While some progress has been made for some of the more intensively studied compound events, for example, extreme temperature and precipitation (AghaKouchak et al., 2014; Turner et al., 2019), there is a real dearth of evidence for the less common events. This paper, in providing the first analysis of projected changes in compound events and exposed population in Africa, provides a solid foundation upon which the consideration of compound events in climate risk assessments at the continental and regional level can begin, such that a more complete picture of the climate risks that Africa may face can start to be established, and more effective adaptation policies developed.

Acknowledgments

The authors would like to thank the Copernicus Climate Change Service for providing the ERA5 reanalysis data set (<https://climate.copernicus.eu/climate-reanalysis>). We acknowledge that this work contains modified Copernicus Climate Change Service Information (2019) and neither the European Commission nor ECMWF is responsible for any use that may be made of the Copernicus information or data it contains. Furthermore, we would like to thank the World Climate Research Program Working Group on Coupled Modelling and all the modeling groups for computing and providing the CMIP5 simulations used as forcing data as well as the Coordinated Regional Downscaling Experiment (CORDEX) framework and Coordinated Output for Regional Evaluations (CORE). We acknowledge the Inter-Sectoral Impact Model Intercomparison Project for providing the annual historical population (ISIMIP2b, <https://www.isimip.org/gettingstarted/details/31>) and the Deutsche Klimarechenzentrum (DKRZ) in Hamburg for providing the high-computing capacity. Moreover, we would like to thank the Earth System Grid Federation (ESGF) for hosting the CORDEX-CORE projections (<https://esgf-data.dkrz.de/projects/esgf-dkrz/>), the Potsdam-Institute for Climate Impact Research for hosting the ISIMIP2b data (<https://esg.pik-potsdam.de/projects/isimip/>), and the NASA Socioeconomic Data and Applications Center (SEDAC) for providing the population projections based on the Shared Socioeconomic Pathways (SSPs) (<https://sedac.ciesin.columbia.edu/>). We are grateful for the support of the all GERICS and ICTP colleagues that made this work possible. Finally, we would like also to thank the anonymous reviewers who helped to improve this study. Open access funding enabled and organized by Projekt DEAL.

References

Abba Omar, S., & Abiodun, B. J. (2017). How well do CORDEX models simulate extreme rainfall events over the East Coast of South Africa? *Theoretical and Applied Climatology*, 128, 453–464. <https://doi.org/10.1007/s00704-015-1714-5>

AghaKouchak, A., Cheng, L., Mazdiyasi, O., & Farahmand, A. (2014). Global warming and changes in risk of concurrent climate extremes: Insights from the 2014 California drought. *Geophysical Research Letters*, 41, 8847–8852. <https://doi.org/10.1002/2014GL062308>

Ahmadalipour, A., Moradkhani, H., Castelletti, B., & Magliocca, N. (2019). Future drought risk in Africa: Integrating vulnerability, climate change, and population growth. *Science of the Total Environment*, 662, 672–686. <https://doi.org/10.1016/j.scitotenv.2019.01.278>

Asefi-Najafabady, S., Vandekar, K. L., Seimon, A., Lawrence, P., & Lawrence, D. (2018). Climate change, population, and poverty: Vulnerability and exposure to heat stress in countries bordering the Great Lakes of Africa. *Climatic Change*, 148, 561–573. <https://doi.org/10.1007/s10584-018-2211-5>

Baldwin, J. W., Dessy, J. B., Vecchi, G. A., & Oppenheimer, M. (2019). Temporally compound heat wave events and global warming: An emerging hazard. *Earth's Future*, 7, 411–427. <https://doi.org/10.1029/2018EF000989>

Chersich, M. F., Wright, C. Y., Venter, F., Rees, H., Scorgie, F., & Erasmus, B. (2018). Impacts of climate change on health and wellbeing in South Africa. *International Journal of Environmental Research and Public Health*, 15, 1884. <https://doi.org/10.3390/ijerph15091884>

Ciarlo, J. M., Coppola, E., Fantini, A., Giorgi, F., Gao, X., Tong, Y., et al. (2020). A new spatially distributed added value index for regional climate models: the EURO-CORDEX and the CORDEX-CORE highest resolution ensembles. *Climate Dynamics*. <https://doi.org/10.1007/s00382-020-05400-5>

Coffel, E. D., Horton, R. M., & de Sherbinin, A. (2018). Temperature and humidity based projections of a rapid rise in global heat stress exposure during the 21st century. *Environmental Research Letters*, 13(1), 014001. <https://doi.org/10.1088/1748-9326/aaa00e>

Copernicus Climate Change Service (C3S) (2017). ERA5: Fifth generation of ECMWF atmospheric reanalyses of the global climate. Copernicus Climate Change Service Climate Data Store (CDS), Nov. 2019. <https://cds.climate.copernicus.eu/cdsapp#!/home>

Coppola, E., Giorgi, F., Raffaele, F., Fuentes-Franco, R., Giuliani, G., Llopart-Pereira, M., et al. (2014). Present and future climatologies in the Phase I CREMA experiment. *Climatic Change*, 125, 23–38. <https://doi.org/10.1007/s10584-014-1137-9>

Diallo, I., Giorgi, F., Sukumaran, S., Stordal, F., & Giuliani, G. (2015). Evaluation of RegCM4 driven by CAM4 over Southern Africa: Mean climatology, interannual variability and daily extremes of wet season temperature and precipitation. *Theoretical and Applied Climatology*, 121, 749–766. <https://doi.org/10.1007/s00704-014-1260-6>

Diaso, U., & Abiodun, B. J. (2017). Drought modes in West Africa and how well CORDEX RCMs simulate them. *Theoretical and Applied Climatology*, 128, 223–240. <https://doi.org/10.1007/s00704-015-1705-6>

Dosio, A. (2017). Projection of temperature and heat waves for Africa with an ensemble of CORDEX Regional Climate Models. *Climate Dynamics*, 49(1-2), 493–519. <https://doi.org/10.1007/s00382-016-3355-5>

Endris, H. S., Omondi, P., Jain, S., Lennard, C., Hewitson, B., Chang'a, L., et al. (2013). Assessment of the performance of CORDEX regional climate models in simulating East African rainfall. *Journal of Climate*, 26, 8453–8475. <https://doi.org/10.1175/JCLI-D-12-00708.1>

Feng, S., Hao, Z., Zhang, X., & Hao, F. (2019). Probabilistic evaluation of the impact of compound dry-hot events on global maize yields. *Science of the Total Environment*, 689, 1228–1234. <https://doi.org/10.1016/j.scitotenv.2019.06.373>

Fotso-Nguemo, T. C., Vondou, D. A., Pokam, W. M., Djomou, Z. Y., Diallo, I., Haensler, A., et al. (2017). On the added value of the regional climate model REMO in the assessment of climate change signal over Central Africa. *Climate Dynamics*, 49, 3813–3838. <https://doi.org/10.1007/s00382-017-3547-7>

- Fotso-Nguemo, T. C., Vondou, D. A., Tchawoua, C., & Haensler, A. (2017). Assessment of simulated rainfall and temperature from the regional climate model REMO and future changes over Central Africa. *Climate Dynamics*, *48*, 3685–3705. <https://doi.org/10.1007/s00382-016-3294-1>
- Giorgi, F., Coppola, E., Raffaele, F., Diro, G. T., Fuentes-Franco, R., Giuliani, G., et al. (2014). Changes in extremes and hydroclimatic regimes in the CREMA ensemble projections. *Climatic Change*, *125*, 39–51. <https://doi.org/10.1007/s10584-014-1117-0>
- Giorgi, F., Coppola, E., Solmon, F., Mariotti, L., Sylla, M. B., Bi, X., et al. (2012). RegCM4: Model description and preliminary tests over multiple CORDEX domains. *Climate Research*, *52*(1), 7–29. <https://doi.org/10.3354/cr01018>
- Hao, Z., Hao, F., Singh, V. P., & Zhang, X. (2018). Changes in the severity of compound drought and hot extremes over global land areas. *Environmental Research Letters*, *13*, 124022. <https://doi.org/10.1088/1748-9326/aeee96>
- Harrington, L. J., & Otto, F. E. L. (2018). Changing population dynamics and uneven temperature emergence combine to exacerbate regional exposure to heat extremes under 1.5°C and 2°C of warming. *Environmental Research Letters*, *13*, 034011. <https://doi.org/10.1088/1748-9326/aaaa99>
- He, X., & Sheffield, J. (2020). Lagged compound occurrence of droughts and pluvials globally over the past seven decades. *Geophysical Research Letters*, *47*, e2020GL087924. <https://doi.org/10.1029/2020GL087924>
- Hendry, A., Haigh, I. D., Nicholls, R. J., Winter, H., Neal, R., Wahl, T., et al. (2019). Assessing the characteristics and drivers of compound flooding events around the UK coast. *Hydrology and Earth System Sciences*, *23*, 3117–3139. <https://doi.org/10.5194/hess-23-3117-2019>
- Hoegh-Guldberg, O., Jacob, D., Taylor, M., Guillén Bolaños, T., Bindi, M., Brown, S., et al. (2019). The human imperative of stabilizing global climate change at 1.5°C. *American Association for the Advancement of Science*, *365*(6459), eaaw6974. <https://doi.org/10.1126/science.aaw6974>
- Hummel, M., Hallahan, B. F., Brychkova, G., Ramirez-Villegas, J., Guwela, V., Chataika, B., et al. (2018). Reduction in nutritional quality and growing area suitability of common bean under climate change induced drought stress in Africa. *Scientific Reports*, *8*, 16187. <https://doi.org/10.1038/s41598-018-33952-4>
- Iturbide, M., Gutiérrez, J. M., Alves, L., Bedia, J., Cerezo-Mota, R., Di Luca, A., et al. (2020). An update of IPCC physical climate reference regions for subcontinental analysis of climate model data: Definition and aggregated datasets. *Earth System Science Data Discussions*, in review, 2020. <https://doi.org/10.5194/essd-2019-258>
- Jacob, D., Elizalde, A., Haensler, A., Hagemann, S., Kumar, P., Podzun, R., et al. (2012). Assessing the transferability of the regional climate model REMO to different coordinated regional climate downscaling experiment (CORDEX) regions. *Atmosphere*, *3*(1), 181–199. <https://doi.org/10.3390/atmos3010181>
- Jones, B., & O'Neill, B. C. (2016). Spatially explicit global population scenarios consistent with the shared socioeconomic pathways. *Environmental Research Letters*, *11*, 084003. <https://doi.org/10.1088/1748-9326/11/8/084003>
- Jones, B., & O'Neill, B. C. (2017). Global population projection grids based on shared socioeconomic pathways (SSPs), 2010–2100. Palisades, NY: NASA Socioeconomic Data and Applications Center (SEDAC). <https://doi.org/10.7927/H4RF5S0P>. Accessed 23 Sept. 2019.
- Jones, B., O'Neill, B. C., McDaniel, L., McGinnis, S., Mearns, L. O., & Tebaldi, C. (2015). Future population exposure to US heat extremes. *Nature Climate Change*, *5*(7), 652–655. <https://doi.org/10.1038/nclimate2631>
- Kendon, E. J., Stratton, R. A., Tucker, S., Marsham, J. H., Berthou, S., Rowell, D. P., & Senior, C. A. (2019). Enhanced future changes in wet and dry extremes over Africa at convection-permitting scale. *Nature Communications*, *10*, 1794. <https://doi.org/10.1038/s41467-019-09776-9>
- Klutse, N. A. B., Sylla, M. B., Diallo, I., Sarr, A., Dosio, A., Diedhiou, A., et al. (2016). Daily characteristics of West African summer monsoon precipitation in CORDEX simulations. *Theoretical and Applied Climatology*, *123*, 369–386. <https://doi.org/10.1007/s00704-014-1352>
- Leonard, M., Westra, S., Phatak, A., Lambert, M., van den Hurk, B., McInnes, K., et al. (2014). A compound event framework for understanding extreme impacts. *WIREs Climate Change*, *5*, 113–128. <https://doi.org/10.1002/wcc.252>
- Liu, Z., Anderson, B., Yan, K., Dong, W., Liao, H., & Shi, P. (2017). Global and regional changes in exposure to extreme heat and the relative contributions of climate and population change. *Scientific Reports*, *7*, 1, 43909–9. <https://doi.org/10.1038/srep43909>
- Lu, Y., Hu, H., Li, C., & Tian, F. (2018). Increasing compound events of extreme hot and dry days during growing seasons of wheat and maize in China. *Scientific Reports*, *8*, 16700. <https://doi.org/10.1038/s41598-018-34215-y>
- Manning, C., Widmann, M., Bevacqua, E., Van Loon, A. F., Maraun, D., & Vrac, M. (2019). Increased probability of compound long-duration dry and hot events in Europe during summer (1950–2013). *Environmental Research Letters*, *14*, 094006. <https://doi.org/10.1088/1748-9326/ab23bf>
- Martius, O., Pfahl, S., & Chevalier, C. (2016). A global quantification of compound precipitation and wind extremes. *Geophysical Research Letters*, *43*, 7709–7717. <https://doi.org/10.1002/2016GL070017>
- Matthews, T., Wilby, R. L., & Murphy, C. (2019). An emerging tropical cyclone-deadly heat compound hazard. *Nature Climate Change*, *9*, 602–606. <https://doi.org/10.1038/s41558-019-0525-6>
- Mazdiyasi, O., & AghaKouchak, A. (2015). Substantial increase in concurrent droughts and heatwaves in the United States. *PNAS*, *112*, 11,484–11,489. <https://doi.org/10.1073/pnas.1422945112>
- Moftakhari, H., & AghaKouchak, A. (2019). Increasing exposure of energy infrastructure to compound hazards: Cascading wildfires and extreme rainfall. *Environmental Research Letters*, *14*, 104018. <https://doi.org/10.1088/1748-9326/ab41a6>
- Moss, R. H., Edmonds, J. A., Hibbard, K. A., Manning, M. R., Rose, S. K., Van Vuuren, D. P., et al. (2010). The next generation of scenarios for climate change research and assessment. *Nature*, *463*(7282), 747–756. <https://doi.org/10.1038/nature08823>
- Muccione, V., Allen, S., Huggel, C., & Birkmann, J. (2016). Differentiating regions for adaptation financing: The role of global vulnerability and risk distributions. *Wiley Interdisciplinary Reviews: Climate Change*, *8*, WCC477. <https://doi.org/10.1002/wcc.447>
- Niang, I., Ruppel, O. C., Abdrabo, M. A., Essel, A., Lennard, C., Padgham, J., & Urquhart, P. (2014). Africa. In V. R. Barros, et al. (Eds.), *Climate change 2014: Impacts, adaptation, and vulnerability. Part B: Regional Aspects. Contribution of Working Group II to the Fifth Assessment Report of the Intergovernmental Panel on Climate Change* (pp. 1199–1265). Cambridge, United Kingdom and New York, NY, USA: Cambridge University Press.
- Ogwang, B. A., Chen, H., Li, X., & Gao, C. (2016). Evaluation of the capability of RegCM4.0 in simulating East African climate. *Theoretical and Applied Climatology*, *124*, 303–313. <https://doi.org/10.1007/s00704-015-1420-3>
- Remedio, A. R., Teichmann, C., Buntmeyer, L., Sieck, K., Weber, T., Rechid, D., et al. (2019). Evaluation of new CORDEX simulations using an updated Köppen-Trewartha climate classification. *Atmosphere*, *10*, 726. <https://doi.org/10.3390/atmos10110726>
- Rohat, G., Flacke, J., Dosio, A., Dao, H., & van Maarseveen, M. (2019). Projections of human exposure to dangerous heat in African cities under multiple socioeconomic and climate scenarios. *Earth's Future*, *7*, 528, 2018EF001020–546. <https://doi.org/10.1029/2018EF001020>
- Russo, S., Marchese, A. F., & Sillmann, J. (2016). When will unusual heat waves become normal in a warming Africa? *Environmental Research Letters*, *11*, 054016. <https://doi.org/10.1088/1748-9326/11/5/054016>

- Russo, S., Sillmann, J., Sippel, S., Barcikowska, M. J., Ghisetti, C., Smid, M., & O'Neill, B. (2019). Half a degree and rapid socioeconomic development matter for heatwave risk. *Nature Communications*, *10*, 136. <https://doi.org/10.1038/s41467-018-08070-4>
- Sadegh, M., Moftakhari, H., Gupta, H. V., Ragno, E., Mazdiyasn, O., Sanders, B., et al. (2018). Multihazard scenarios for analysis of compound extreme events. *Geophysical Research Letters*, *45*, 5470–5480. <https://doi.org/10.1029/2018GL077317>
- Sedlmeier, K., Feldmann, H., & Schädler, G. (2018). Compound summer temperature and precipitation extremes over central Europe. *Theoretical and Applied Climatology*, *131*, 1493–1501. <https://doi.org/10.1007/s00704-017-2061-5>
- Sedlmeier, K., Mieruch, S., Schädler, G., & Kottmeier, C. (2016). Compound extremes in a changing climate—A Markov chain approach. *Nonlinear Processes in Geophysics*, *23*, 375–390. <https://doi.org/10.5194/npg-23-375-2016>
- Seneviratne, S. I., Nicholls, N., Easterling, D., Goodess, C. M., Kanae, S., Kossin, J., et al. (2012). Changes in climate extremes and their impacts on the natural physical environment. In C. B. Field, et al. (Eds.), *Managing the Risks of Extreme Events and Disasters to Advance Climate Change Adaptation. A Special Report of Working Groups I and II of the Intergovernmental Panel on Climate Change (IPCC)* (pp. 109–230). Cambridge, UK, and New York, NY, USA: Cambridge Univ. Press, 2012, chap. 3.
- Stern, P. C., Ebi, K. L., Leichenko, R., Olson, R. S., Steinbruner, J. D., & Lempert, R. (2013). Managing risk with climate vulnerability science. *Nature Climate Change*, *3*, 607–609. <https://doi.org/10.1038/nclimate1929>
- Tamoffo, A. T., Vondou, D. A., Pokam, W. M., Haensler, A., Yepdo, Z. D., Fotso-Nguemo, T. C., et al. (2019). Daily characteristics of Central African rainfall in the REMO model. *Theoretical and Applied Climatology*, *137*, 2351–2368. <https://doi.org/10.1007/s00704-018-2745-5>
- Tang, C., Morel, B., Wild, M., Pohl, B., Abiodun, B., & Bessafi, M. (2019). Numerical simulation of surface solar radiation over Southern Africa. Part 1: Evaluation of regional and global climate models. *Climate Dynamics*, *52*, 457–477. <https://doi.org/10.1007/s00382-018-4143-1>
- Taylor, K. E., Stouffer, R. J., & Meehl, G. A. (2012). An overview of CMIP5 and the experiment design. *Bulletin of the American Meteorological Society*, *93*(4), 485–498. <https://doi.org/10.1175/BAMS-D-11-00094.1>
- Teichmann, C., Eggert, B., Elizalde, A., Haensler, A., Jacob, D., Kumar, P., et al. (2013). How does a regional climate model modify the projected climate change signal of the driving GCM: A study over different CORDEX regions using REMO. *Atmosphere*, *4*, 214–236. <https://doi.org/10.3390/atmos4020214>
- Tencer, B., Bettolli, M. L., & Rusticucci, M. (2016). Compound temperature and precipitation extreme events in Southern South America: associated atmospheric circulation and simulations by a multi-RCM ensemble. *Climate Research*, *68*, 183–199. <https://doi.org/10.3354/cr01396>
- Thomas, K., Hardy, R. D., Lazrus, H., Mendez, M., Orlove, B., Rivera-Collazo, I., et al. (2018). Explaining differential vulnerability to climate change: A social science review. *WIREs Climate Change*, *10*(2). <https://doi.org/10.1002/wcc.565>
- Thornton, P. K., Jones, P. J., Ericksen, P. J., & Challinor, A. J. (2011). Agriculture and food systems in sub-Saharan Africa in a 4°C + world. *Philosophical Transactions of the Royal Society A*, *369*(1934), 117–136. <https://doi.org/10.1098/rsta.2010.0246>
- Turner, S. W. D., Voisin, N., Fazio, J., Hua, D., & Jourabchi, M. (2019). Compound climate events transform electrical power shortfall risk in the Pacific Northwest. *Nature Communications*, *10*, 8. <https://doi.org/10.1038/s41467-018-07894-4>
- United Nations, Department of Economic and Social Affairs, Population Division (2019). *World Population Prospects 2019: Highlights (ST/ESA/SER.A/423)*.
- Wahl, T., Jain, S., Bender, J., Meyers, S. D., & Luther, M. E. (2015). Increasing risk of compound flooding from storm surge and rainfall for major US cities. *Nature Climate Change*, *5*, 1093–1097. <https://doi.org/10.1038/nclimate2736>
- Weber, T., Haensler, A., Rechid, D., Pfeifer, S., Eggert, B., & Jacob, D. (2018). Analyzing Regional Climate Change in Africa in a 1.5, 2, and 3°C Global Warming World. *Earth's Future*, *6*, 643–655. <https://doi.org/10.1002/2017EF000714>
- Williges, K., Mechler, R., Bowyer, P., & Balkovič, J. (2017). Towards an assessment of adaptive capacity of the European agricultural sector to droughts. *Climate Services*, *7*, 47–63. <https://doi.org/10.1016/j.cliser.2016.10.003>
- Wu, X., Hao, Z., Hao, F., Li, C., & Zhang, X. (2019). Spatial and temporal variations of compound droughts and hot extremes in China. *Atmosphere*, *10*, 95. <https://doi.org/10.3390/atmos10020095>
- Ye, L., Shi, K., Xin, Z., Wang, C., & Zhang, C. (2019). Compound droughts and heat waves in China. *Sustainability*, *11*, 3270. <https://doi.org/10.3390/su11123270>
- Zscheischler, J., Martius, O., Westra, S., Bevacqua, E., Raymond, C., Horton, R. M., et al. (2020). A typology of compound weather and climate events. *Nature Reviews Earth & Environment*, *1*(7), 333–347. <https://doi.org/10.1038/s43017-020-0060-z>
- Zscheischler, J., & Seneviratne, S. I. (2017). Dependence of drivers affects risks associated with compound events. *Science Advances*, *3*, e1700263. <https://doi.org/10.1126/sciadv.1700263>
- Zscheischler, J., Westra, S., Van Den Hurk, B. J. J. M., Seneviratne, S. I., Ward, P. J., Pitman, A., et al. (2018). Future climate risk from compound events. *Nature Climate Change*, *8*, 469–477. <https://doi.org/10.1038/s41558-018-0156-3>